

Article

Not peer-reviewed version

Accurate Determination of the Temperature Sensitivity of UV-Induced Fiber Bragg Gratings

[Miguel Cosme](#) , [Marizane Pota](#) , João Preizal , [Paulo Caldas](#) , [Ricardo Oliveira](#) , [Rogério Nogueira](#) , Francisco M. Araújo , [José Luis Cruz](#) , [Gaspar M. Rego](#) *

Posted Date: 28 November 2025

doi: 10.20944/preprints202511.2298.v1

Keywords: Fiber Bragg gratings; temperature sensitivity



Preprints.org is a free multidisciplinary platform providing preprint service that is dedicated to making early versions of research outputs permanently available and citable. Preprints posted at Preprints.org appear in Web of Science, Crossref, Google Scholar, Scilit, Europe PMC.

Copyright: This open access article is published under a [Creative Commons CC BY 4.0 license](#), which permit the free download, distribution, and reuse, provided that the author and preprint are cited in any reuse.

Disclaimer/Publisher's Note: The statements, opinions, and data contained in all publications are solely those of the individual author(s) and contributor(s) and not of MDPI and/or the editor(s). MDPI and/or the editor(s) disclaim responsibility for any injury to people or property resulting from any ideas, methods, instructions, or products referred to in the content.

Article

Accurate Determination of the Temperature Sensitivity of UV-Induced Fiber Bragg Gratings

Miguel Cosme ¹, Marizane Pota ², João Preizal ³, Paulo Caldas ^{4,5}, Ricardo Oliveira ³, Rogério Nogueira ³, Francisco M. Araújo ¹, José L. Cruz ⁶ and Gaspar M. Rego ^{2,4,*}

¹ HBK FiberSensing, S. A., Maia, Portugal

² ADiT-LAB, Instituto Politécnico de Viana do Castelo, *Rua Escola Industrial e Comercial Nun'Álvares*, 4900-347 Viana do Castelo, Portugal

³ Instituto de Telecomunicações and University of Aveiro, Campus Universitário de Santiago, 3810-1938 Aveiro, Portugal

⁴ Center for Applied Photonics, INESC TEC, Rua Dr. Roberto Frias, 4200-465 Porto, Portugal

⁵ CISAS, Escola Superior de Tecnologia e Gestão, Instituto Politécnico de Viana do Castelo

⁶ Universidad de Valencia, Department of Applied Physics, Dr. Moliner 50, Burjassot 46100, Valencia, Spain

* Correspondence: gaspar@estg.ipv.pt

Abstract

Over the past 18 months, we have performed hundreds of temperature characterizations of fiber Bragg gratings inscribed in different germanium-doped silica glass fibers. Under the experimental conditions, the main conclusions, are: the temperature dependence of the “temperature gauge factor” or the normalized temperature sensitivity, K_T , was found to be quadratic in the -50 – 200 °C range while it may be considered linear for the -20 – 100 °C range; K_T values at 20 °C varies from 5.176×10^{-6} K⁻¹, for a B/Ge co-doped fiber up to 6.724×10^{-6} K⁻¹, for a highly Ge-doped fiber; K_T does not depend on the hydrogen-loading process or the gratings coupling strength; K_T is essentially independent on wavelength in the 1500 – 1600 nm range being its value accurately determined with a relative error $\sim 0.2\%$; gratings produced by femtosecond-laser radiation and UV-laser radiation exhibit comparable values of K_T . The previous achievements allows, by having knowledge of K_T for a single grating, the accurate determination of the temperature dependence of the Bragg wavelength for any other grating inscribed in the same fiber; the presented methodology enables one to determine the “unknown” gratings temperature sensitivity, typically, with an error of 0.01 pm/°C, being, therefore, very useful in research labs and computer simulations; thus, expressions for the temperature dependence of K_T for gratings inscribed in several fibers are given. We have also fully analyzed the potential sources of error in K_T determination.

Keywords: Fiber Bragg gratings; temperature sensitivity

1. Introduction

For more than three decades, temperature sensing is being, probably, the most well-known application of fiber Bragg gratings (FBG) [1–6]. Independently of the physical parameter under measurement, temperature discrimination is required [7–12]. In this context, a precise determination of temperature is an essential task and, therefore, an accurate knowledge of the FBG temperature sensitivity is on demand [13]. In comparison to the number of publications related to FBG theory, applications and simulations, only few acknowledge the fact that the Bragg wavelength shifts nonlinearly with temperature, even for a limited temperature range, such as 120 °C, and that the thermo-optic coefficient of silica-doped glass fibers depends on temperature and wavelength [13–16]. Recently [16], preliminary results pointed toward the independence on wavelength of the “temperature gauge factor” $K_T=(1/\lambda)(d\lambda/dT)$ [17] or the normalized temperature sensitivity, in the 1500 – 1600 nm range. However, we recognize that definite conclusions require higher stability,

accuracy and resolution of the equipment used. Therefore, in this paper we compare the normalized temperature sensitivity of fs-FBG and UV-FBG, we discuss the potential effect of the hydrogen-loading process and of the initial grating coupling strength on K_T values. We demonstrate that K_T is, essentially, independent on wavelength in the 1500–1600 nm wavelength range. Based on the previous results, we also demonstrate that the temperature dependence of the Bragg wavelength of a second FBG can be predicted through integration of the K_T expression obtained previously for a former FBG. A thorough discussion on the experimental errors that can affect the determination of the FBG temperature sensitivity is also presented. The K_T expressions for FBG inscribed in silica fibers with distinct concentrations of GeO_2 are also given.

2. Gratings Fabrication

The UV-FBGs were inscribed in six different fibers: Corning SMF-28 (NA=0.14) and SMF-28e+ (NA=0.14), Leoni SMF with an Ormocer coating (NA=0.14, MFD=8.8±0.5), FiberCore SM1500 (a high GeO_2 -dopant concentration having NA: 0.19-0.21 and 0.29-0.31), and FiberCore PS1250/1500 (a B/Ge co-doped fiber having NA: 0.12-0.14). Gratings were made by scanning a UV laser (244 nm, laser beam cross section= 0.9*0.9 mm²) over the fibers through a phase mask Ibsen Photonics® (period = 1063.50 nm and length = 10 mm), as depicted in Figure 1. Different grating strengths were achieved by changing several parameters. For the specific gratings produced (PS1250/1500 and SM1500 fibers) the laser power has been in the range 10 mW to 70 mW, the beam scanning speed in the range 0.01685 mm/s to 1.348 mm/s. Gratings in the PS 1250/1500 fiber and grating of 33% reflectivity (R) in the SM1500 fiber were made without focusing lens. Gratings with R=12%, 2.8% and 0.7% in SM1500 fiber (NA: 0.29-0.31) were made with divergent cylindric lens (intensity in the fiber decreased by a factor of 10), and the phase mask period was 1056.50 nm (Table 1). Note that the choice of the phase mask period, Λ , was such that the Bragg wavelength ($\lambda_B = n_{\text{eff}}\Lambda$, being n_{eff} the effective refractive index) would be in the 1500-1600 nm range.

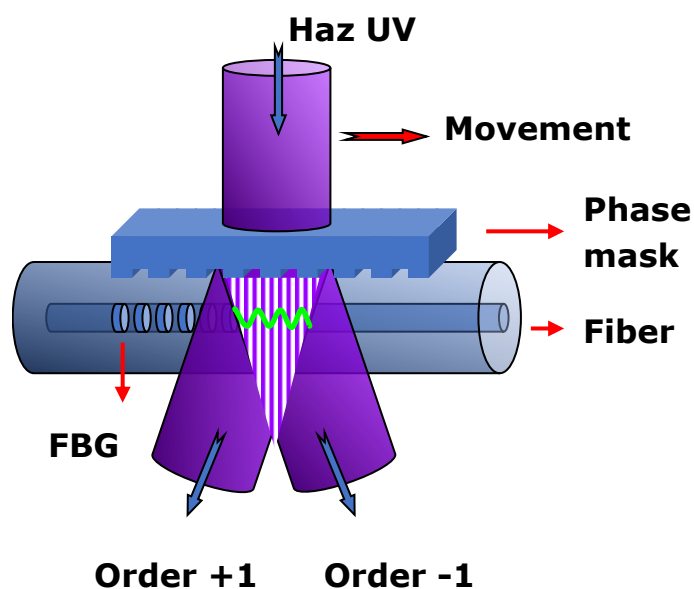


Figure 1. Schematic of the fiber Bragg grating recording system based on the phase mask method.

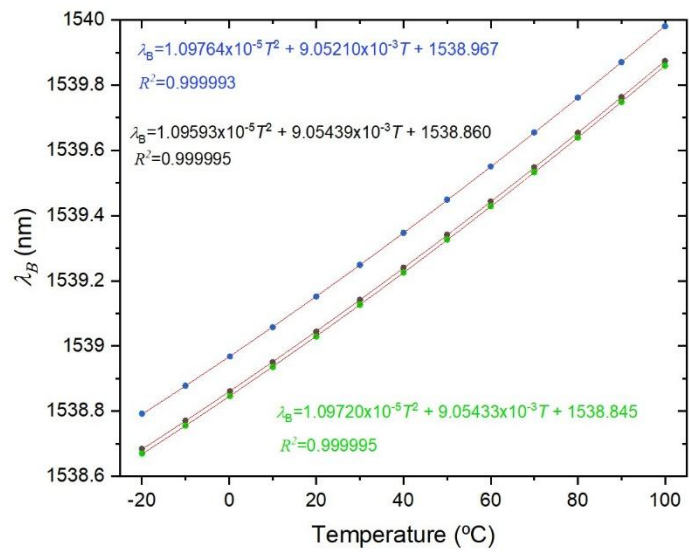
Table 1. Gratings reflectivity and UV fluence for the gratings inscribed in six different fibers.

SMF-28e+ pristine	SMF-28e+ H ₂ loaded	SM1500 NA=0.29-0.31	PS1250/1500, NA=0.12-0.14
R (%) / E'' (J/mm ²)	R (%) / E'' (J/mm ²)	R (%) / E'' (J/mm ²)	R (%) / E'' (J/mm ²)
7.3 / 48.8	15 / 3.30	33 / 0.857	13 / 2.308

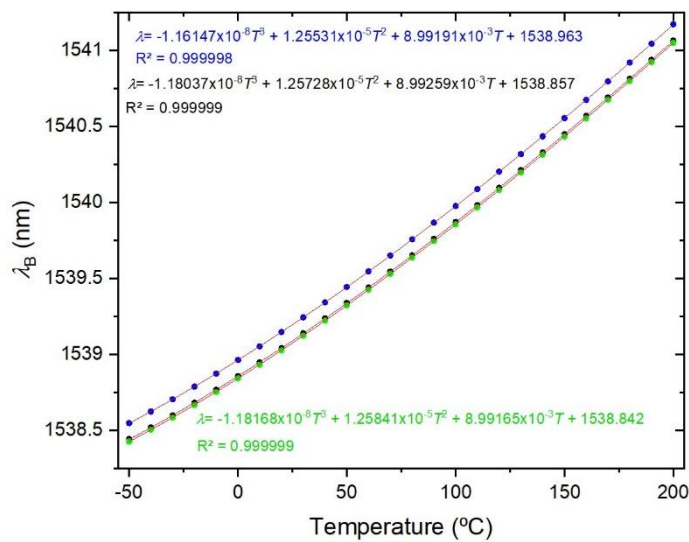
1.2	9.76	4	1.32	12	0.429	4	0.923
0.36	4.62	1.3	0.264	2.8	0.00536	1.5	0.154
0.07	0.923	0.095	0.0528	0.7	0.00165	0.26	0.0264
SMF-28	Leoni SMF w/Ormocer coating			SM1500 NA=0.19-0.21			
R (%) / E'' (J/mm ²)	R (%) / E'' (J/mm ²)			R (%) / E'' (J/mm ²)			
1.6	9.89	---	9.89	10	0.923		
0.46	4.94	---	4.94	1.0	0.0923		
0.09	0.989	---	0.989	0.51	0.00385		

3. Gratings Thermal Characterization

The temperature characterization was performed using a Dry block-temperature calibrator from Sika, model type TP17200S, allowing measurements between $-55\text{ }^{\circ}\text{C}$ and $200\text{ }^{\circ}\text{C}$ with $0.01\text{ }^{\circ}\text{C}$ resolution and an accuracy of $0.2\text{ }^{\circ}\text{C}$. Gratings were mounted inside the insert blocks keeping them stress-free. Bragg wavelengths were measured, after $\sim 1\text{h}$ stabilization, using an optical interrogator FS22SI BraggMeter ST (with 8 channels), with an acquisition rate of 1 sample/s, which enables resolution/stability better than $0.5\text{ pm}/1\text{ pm}$. The temperature range was from $-20\text{ }^{\circ}\text{C}$ up to $100\text{ }^{\circ}\text{C}$ (cycle: $30\text{ }^{\circ}\text{C}$ up to $90\text{ }^{\circ}\text{C}$, followed by $100\text{ }^{\circ}\text{C}$ down to $-20\text{ }^{\circ}\text{C}$, and finally -10 up to $30\text{ }^{\circ}\text{C}$, all in steps of $20\text{ }^{\circ}\text{C}$). At each temperature step, the Bragg wavelength was determined by averaging 2500 data points and the standard deviation was lower than 0.7 pm , with a typical value of 0.4 pm . A quadratic fitting was applied to the temperature dependence of the Bragg wavelength and it was observed that K_T shifted linearly with temperature. Similarly, gratings inscribed in the SMF-28 fiber were submitted to four heating cycles from $-50\text{ }^{\circ}\text{C}$ up to $200\text{ }^{\circ}\text{C}$. A cubic fitting was applied to the temperature dependence of the Bragg wavelength and K_T shifted quadratically with temperature. Figure 2 shows the temperature dependence of the Bragg wavelength for both temperature cycles. The comparison between the fitting of K_T is presented in Figure 3, where it can be observed that a divergence occurs as one approaches the limits of the temperature interval $[-20, 100]\text{ }^{\circ}\text{C}$. This divergence can be explained by the fact that, at room temperature, $K_T = ((1/n_{\text{eff}})(dn_{\text{eff}}/dT) + \alpha_{\text{SiO}_2})$ (the normalized thermo-optic coefficient and the thermal expansion coefficient, respectively) is essentially determined by the temperature behavior of the thermo-optic coefficient (dn_{eff}/dT), a cubic temperature dependence [13,14,18,19]. The calibrations were repeated with all fiber gratings in Table 1 and results are summarized in Table 2. It can be observed that K_T increases with the fiber GeO_2 content, being lower for the B/Ge fiber. The absolute values of K_T for the SMF-28 fiber and Leoni SMF with an Ormocer coating differs from the ones previously measured [16]. Therefore, we performed a reanalysis of those experiments and results will be discussed in the next section. The possible effect of the hydrogen-loading process or the grating coupling strength (reflectivity) on K_T values was studied using gratings in the SMF-28e+ fiber. The results have shown that up to a reflectivity of 15% there is no impact on the determination of the normalized temperature sensitivity. Similar results were obtained for the other fibers, namely, a grating induced in the PS1500 (NA=0.29) fiber with a reflectivity as high as 33% was tested and gratings inscribed in a batch of the Leoni SMF with an Ormocer coating, having reflectivity ranging from 1% up to a saturated level, were also used.



(a)



(b)

Figure 2. Bragg wavelength temperature dependence for the three UV-FBGs induced in the SMF-28 fiber: (a) four heating cycles -20 - 100 $^{\circ}\text{C}$ and (b) four heating cycles -50 - 200 $^{\circ}\text{C}$ (average values for each FBG).

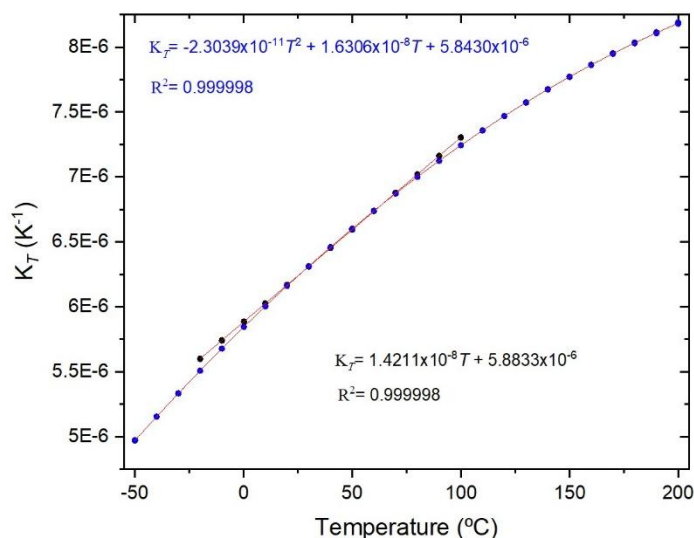


Figure 3. K_T versus temperature (average values) considering the three FBGs for both temperature cycles.

Table 2. K_T expressions for FBG inscribed in different fibers, in the temperature range* [-20, 100] °C.

Fiber	K_T (K ⁻¹) (T is in °C in equations below)	K_T @20 °C
Fibercore PS1250/1500 NA=0.12-0.14	$1.5619 \times 10^{-8} T + 4.8636 \times 10^{-6}$	5.176×10^{-6}
Corning SMF-28 *[-50, 200] °C	$-2.3039 \times 10^{-11} T^2 + 1.6306 \times 10^{-8} T + 5.8430 \times 10^{-6}$	6.166×10^{-6}
Corning SMF-28 limited to [-20, 100] °C	$1.4310 \times 10^{-8} T + 5.8786 \times 10^{-6}$	6.165×10^{-6}
Corning SMF-28e+ NA=0.14	$1.4348 \times 10^{-8} T + 5.8777 \times 10^{-6}$	6.165×10^{-6}
Leoni SMF w/Ormocer coating NA=0.14, MFD=8.8±0.5	$1.4524 \times 10^{-8} T + 5.8956 \times 10^{-6}$	6.186×10^{-6}
Fibercore SM1500 NA=0.19-0.21	$1.5118 \times 10^{-8} T + 5.9358 \times 10^{-6}$	6.238×10^{-6}
Fibercore SM1500 NA=0.29-0.31	$1.5890 \times 10^{-8} T + 6.2564 \times 10^{-6}$	6.574×10^{-6}

4. Error Analysis Related to FBG Thermal Characterization

This section besides the scientific content, also intends to be a pedagogical one in an era of unprecedented exponential increase of “insufficient mature” published data. The initial thermal characterizations were performed using a customized oven as described in [20] (although with shorter dimensions) and the thermal bath described in [16]. However, both heating apparatuses exhibited errors in the absolute temperature measurements. We realized that a 5 pm difference (or equivalently a temperature difference of 0.5 °C) on each temperature step led, after fitting the temperature dependence of the Bragg wavelength, to values of K_T at room temperature (20 °C) that were expected for 29.4 °C, being clearly not sufficient for the precision required [13]. Therefore, all further characterizations were performed using the calibrated Dry block described in the previous section and using this new setup (Dry block + interrogator), we have investigated the potential source of errors in the determination of the temperature dependence of the Bragg wavelength, for which hundreds (above 750) of independent temperature measurements were performed over the last 18 months.

The potential effect of using different optical interrogators (comparison with a FS22SI with 4 channels) was analyzed. We have tested 3 FBG ($\lambda_B \sim 1543$ nm) inscribed in the SM1500 (NA_{0.19}) and other 3 FBG ($\lambda_B \sim 1541$ nm) induced in the Leoni SMF fiber (with an Ormocer coating). Three heating cycles were performed in the temperature interval: -20 - 100 °C, using the 8 channels unit and 4 more for the 4 channels unit in a total of 34 tests. All K_T values at 20 °C were in the interval ± 0.004 K⁻¹, therefore, both interrogators register the same values of Bragg wavelengths and, consequently, leading to the same K_T values. We have identified another source of error related to a temperature gradient inside the calibration inserts (15.0 cm long) containing the FBG, which was estimated to be ~ 0.3 °C/cm outside the homogeneous temperature region. For that we have inserted gratings at different depths (5 to 15 cm) and we have also used an array with five 4.5 mm-gratings separated by ~ 10 mm. The Sika manual states that the homogeneous temperature zone is limited to 4.0 cm, therefore, the FBG should be well inside that region at the bottom of the insert. Since the temperature stability is very important to obtain good measurements, for each temperature step we analyzed the standard deviation, that typically was better than 0.4 pm, and we calculated the average of the resonance wavelength, typically using 2500 data points. When we close the cycle returning to the initial temperature we also checked the resonance wavelength, the difference should be lower than 1 pm. Sometimes the device loses stability, probably associated to condensation, which is observed in Figure 4 (b)-(d) (wavelength vs time) and that also impacts the values obtained for K_T . It should be stressed that we have tried to minimize the occurrence of condensation inside the Dry block by increasing the temperature above 100 °C in the first step before decreasing to 30 °C, but the improvement is not always clear and neither uniform for all channels. The frequency of instability events seems to be associated to changes in temperature and humidity in the lab room along the year. As an example, it was difficult to reach stable values of temperature at -50 °C during summer and, therefore, we limited measurements down to -40 °C.

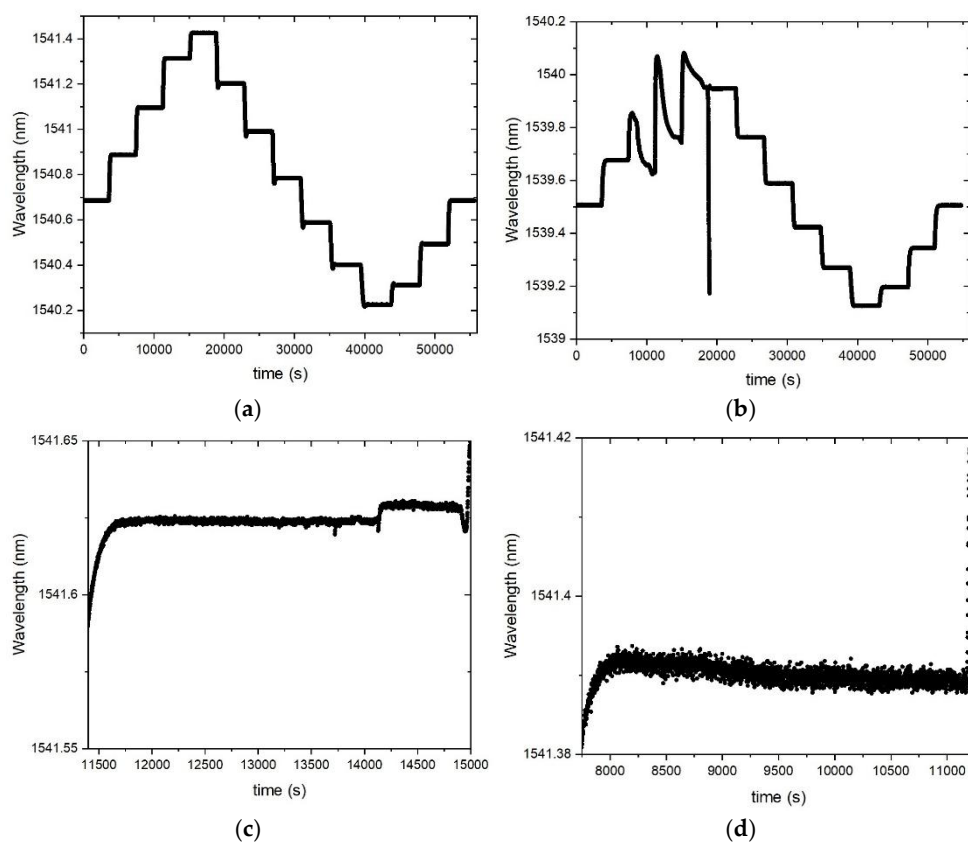


Figure 4. (a) Stable measurements; (b)-(d) instability in one or more temperature steps (initially checked by the larger values of standard deviation).

When the above sources of error are controlled, we still have to deal with the curve fitting. A thorough study on the measurements repeatability was performed by using three gratings inscribed in the SMF-28 fiber. Four heating cycles (–20–100 °C) followed by another four heating cycles (–50–200 °C) were performed. Recently (6 months interval), five heating cycles (–40–200 °C) were also performed to compare reproducibility (measurements were limited to –40 °C, as mentioned above). For the former a 2nd order polynomial fitting was applied to the temperature dependence of the Bragg wavelength while a wider temperature range demands for a higher polynomial fitting (Figure 2). As can be observed in Figure 3 and Figure 5, the normalized temperature sensitivity value is slightly lower for the latter. Nevertheless, a similar value is obtained when restricted to the same temperature range. It should be mentioned that K_T values at 20 °C do not differ by more than 0.01 in each temperature range, totalizing 39 independent measurements. We have also analyzed the influence of decreasing the temperature step, by performing three tests between –40 °C and 100 °C such that when merged with previous tests results in temperature steps of about 2.5 °C. The K_T values are similar to the ones obtained in previous tests (Linear 2 in Figure 5). In general, gratings in other fibers show similar behavior.

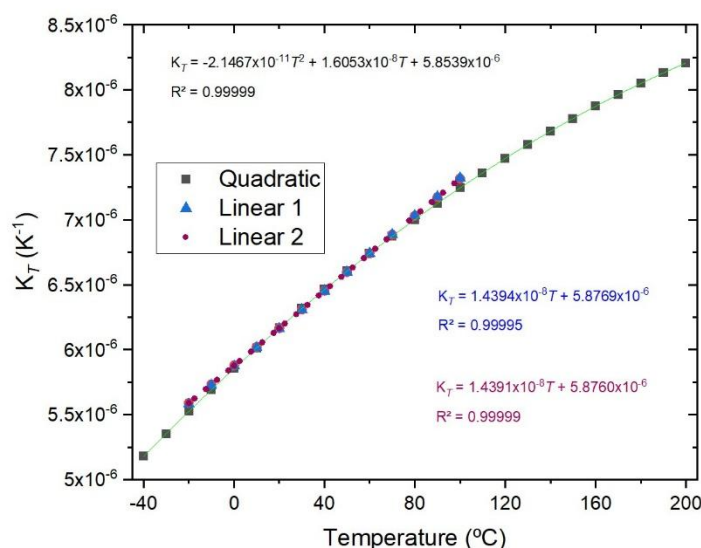


Figure 5. K_T obtained for different temperature ranges and temperature steps.

The last source of error, and one of the most important, is the homogeneity of the fiber itself, that is, the uniform distribution of the germanium concentration along the fiber core. As mentioned previously, we found values for fs-FBG ranging from $6.175 \times 10^{-6} \text{ K}^{-1}$ up to $6.224 \times 10^{-6} \text{ K}^{-1}$, and from $6.153 \times 10^{-6} \text{ K}^{-1}$ up to $6.213 \times 10^{-6} \text{ K}^{-1}$ for UV-FBG. The lack of uniformity was pointed out in the past during the fabrication of mechanically-induced gratings in the SMF-28 fiber [21] and arc-induced gratings in the B/Ge co-doped fiber [22]. In this work, we have used the Leoni SMF fiber as a reference since we had commercially available fs-FBG on it and therefore, we could make comparisons between FBG produced under different fabrication techniques and parameters, such as, reflectivity. Initially we attributed the differences to the fs inscription, but after comparison of UV-FBG produced in the SMF-28 fiber and in the Leoni SMF fiber using different setups ([16] and current work) we notice that while the ones inscribed in the SMF-28 fiber show similar values of K_T , the same did not happen for FBG induced in the Leoni SMF fiber. Moreover, recently we have inscribed FBG in two commercially available batches of SM1500 fiber (both NA=0.19 and NA=0.29) and not only the Bragg wavelength is much higher ($\Delta n_{\text{core}} = 1.555 \times 10^{-3}$ and 4.390×10^{-3} , which corresponds to an estimated increase in GeO₂ concentration of 1.1 and 3.0 mol%, respectively [13]) but also K_T is higher for FBG induced in both fibers: from $6.238 \times 10^{-6} \text{ K}^{-1}$ to $6.290 \times 10^{-6} \text{ K}^{-1}$ and from $6.574 \times 10^{-6} \text{ K}^{-1}$ to 6.724×10^{-6}

K^{-1} , respectively. Therefore, we have used 18 m of the Leoni SMF fiber containing two fs-FBG (~19%; $(6.182 \pm 0.001) \times 10^{-6} \text{ K}^{-1}$) to inscribe UV-FBG with different reflectivity (<1%, 18.9%, 98.8% and saturated) using both setups and all values of K_T fallen in the range: $(6.186 \pm 0.006) \times 10^{-6} \text{ K}^{-1}$. It should be highlighted that peak detection for the high reflectivity gratings is also a demanding task (and the values of R^2 of the fitting are lower for these gratings). Therefore, since we cannot guarantee that there is uniform distribution of germanium in the core of the 18 m of the Leoni SMF fiber, under the experimental conditions, we may conclude that K_T is similar for fs-FBG and UV-FBG and that the coupling strength has negligible influence on the determination of K_T . For the sake of illustration, and since we do not know the fiber parameters in order to determine germanium concentration, we present K_T as a function of n_{eff} in Figure 6. We have also included the K_T value ($K_T = 1.4178 \times 10^{-8} T + 6.1299 \times 10^{-6} \text{ K}^{-1}$; $6.413 \times 10^{-6} \text{ K}^{-1} @ 20^\circ \text{C}$) obtained using three gratings ($\lambda_B \sim 1540, 1547$ and 1554 nm) inscribed in another high Ge-doped fiber (j-fiber SMF: NA=0.26 and MFD=5.5±0.4). It is clearly shown that K_T increases with the increase of GeO_2 concentration and decreases with B_2O_3 concentration.

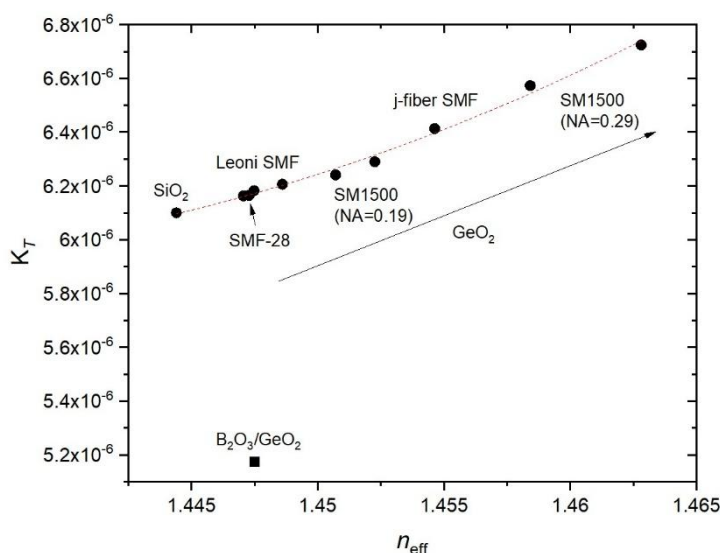


Figure 6. K_T vs n_{eff} @20 °C, obtained for various gratings inscribed in fibers with different germanium concentration.

5. Prediction of the Temperature Dependence of the Bragg Wavelength

Assuming that we know $K(T)$ for one UV-FBG and $\lambda(T_0)$ for a second FBG inscribed in the same fiber, we can determine $\lambda(T)$ for the latter, through integration of $K(T)$ and by applying a 3rd order Taylor expansion to the exponential function. Thus,

$$K(T) = \frac{1}{\lambda} \frac{d\lambda}{dT} = K_2 T^2 + K_1 T + K_0, \quad (1)$$

or

$$K(T) = K_2 (T - T_0)^2 + (K_1 + 2K_2 T_0)(T - T_0) + K(T_0), \quad (2)$$

and therefore,

$$\lambda(T) = \lambda(T_0) * \left[1 + K(T_0) * (T - T_0) + \left(\frac{K_1 + 2K_2 T_0 + K(T_0)^2}{2} \right) * (T - T_0)^2 + \left(\frac{K_2}{3} + \frac{K(T_0)^3}{6} + \frac{(K_1 + 2K_2 T_0) * K(T_0)}{2} \right) * (T - T_0)^3 \right], \quad (3)$$

and

$$\frac{d\lambda(T)}{dT} = \lambda(T_0) * \left[K(T_0) + (K_1 + 2K_2T_0 + K(T_0)^2) * (T - T_0) + \left(K_2 + \frac{K(T_0)^3 + 3(K_1 + 2K_2T_0) * K(T_0)}{2} \right) * (T - T_0)^2 \right], \quad (4)$$

where K_i ($i=0, 1, 2$) are coefficients. For the $[-20, 100]$ temperature range, a linear behavior is adequate and therefore, $K_2=0$. We demonstrate the applicability by using five gratings written in the SM1500 (NA_0.19) fiber with a reflectivity of about 0.5%. Table 3 summarizes the average values of K_T at 20 °C for four tests in the $[-40, 200]$ temperature range, limited to the $[-20, 100]$ °C and also three tests in the $[-20, 97.5]$ °C, in steps of 10 °C but at different temperature plateaus. For each grating, the absolute error of K_T is within 0.002 K^{-1} . Therefore, there is a slight dependence of K_T on wavelength (in a range that exceeds 50 nm) that was averaged in the subsequent calculations. Thus, by fitting all experimental data, for the former temperature range we obtained $K_T = -2.1973 \times 10^{-11} T^2 + 1.6689 \times 10^{-8} T + 5.9194 \times 10^{-6}$ ($R^2 = 0.99998$), for the second $K_T = 1.5004 \times 10^{-8} T + 5.9410 \times 10^{-6}$ ($R^2 = 0.99986$) and for the latter $K_T = 1.5118 \times 10^{-8} T + 5.9358 \times 10^{-6}$ ($R^2 = 0.99985$). Table 4 summarizes the results obtained by comparison of the Bragg wavelengths and temperature sensitivity ($d\lambda/dT$) values from direct calibration ($d\lambda_{dir2}/dT$ and $d\lambda_{dir3}/dT$, for quadratic and cubic fitting, respectively) and by following Eq (1)-(4) where we have assumed K_T through the fitting of all experimental data of the five FBG (λ_{int2} and $d\lambda_{dint2}/dT$, for quadratic fitting and λ_{int3} and $d\lambda_{dint3}/dT$, for cubic fitting). In each temperature range, the difference in wavelength is lower than 3 pm and the calculated temperature sensitivity differs by ~ 0.01 pm/°C. It should be noted that the differences in the temperature sensitivity near the limits of the temperature range (0.1 pm/°C) is essentially due to the dependence of K_T on temperature (goes from quadratic to cubic dependence for larger temperature interval), despite its also slight dependence on wavelength for the five FBG inscribed in this fiber with high GeO₂ dopant concentration (as observed in Table 3 and with impact on the fitting: $R^2 = 0.99986$). Concerning the $[-20, 97.5]$ °C temperature range, the values of K_T at 20 °C have lower dispersion (Table 3) and similar results were obtained when applying the method to estimate the wavelength and temperature sensitivity of the “unknown” grating.

Table 3. K_T values at 20 °C obtained using five FBG induced in the SM1500 (NA_0.19).

λ_B (nm) < K_T (K^{-1})>	1512.7	1527.7	1542.8	1557.7	1565.1
$[-40, 200]$ (°C)	6.248×10^{-6}	6.250×10^{-6}	6.246×10^{-6}	6.239×10^{-6}	6.239×10^{-6}
$[-20, 100]^*$ (°C)	6.244×10^{-6}	6.249×10^{-6}	6.242×10^{-6}	6.237×10^{-6}	6.235×10^{-6}
$[-20, 97.5]$ (°C)	6.242×10^{-6}	6.243×10^{-6}	6.239×10^{-6}	6.233×10^{-6}	6.234×10^{-6}

Table 4. Calculated Bragg wavelength and temperature sensitivity for the “unknown” grating.

T (°C)	$\langle \lambda \rangle$ (nm)	λ_{int2} (nm)	λ_{int3} (nm)	$d\lambda_{int2}/dT$ (pm/°C)	$d\lambda_{dir2}/dT$ (pm/°C)	$d\lambda_{int3}/dT$ (pm/°C)	$d\lambda_{dir3}/dT$ (pm/°C)
-39.94	1527.2213	-----	1527.2195	-----	-----	7.97	7.98
-20	1527.3844	1527.3825	1527.3840	8.62	8.63	8.52	8.53
0.1	1527.5608	1527.5603	1527.5605	9.08	9.09	9.05	9.05
20	1527.7455	1527.7455	1527.7455	9.54	9.55	9.54	9.55
100	1528.5831	1528.5819	1528.5806	11.37	11.38	11.27	11.27
200	1529.7931	-----	1529.7905	-----	-----	12.82	12.81

A similar analysis was performed using five gratings inscribed in the SMF-28 fiber and K_T was calculated in the -20 – 100 °C temperature range. Table 5 summarizes the average values of $d\lambda/dT$ and

K_T for four independent measurements. Note that the dependence of the temperature sensitivity on wavelength is well expressed in Eq. (4). All results are within $6.165 \pm 0.004 \text{ K}^{-1}$, being more stable than the ones obtained for the previous gratings inscribed in the SM1500 fiber. Table 6 shows the results of considering the methodology by using $K_T = 1.4236 \times 10^{-8}T + 5.8831 \times 10^{-6}$ ($R^2 = 0.9999999$) for the FBG at 1509.2 nm and by applying it to the FBG at 1561.6 nm. The largest difference, 2.4 pm, occurs at $-20 \text{ }^\circ\text{C}$ but the sensitivity is always within $0.01 \text{ pm}/^\circ\text{C}$. Similar results would be obtained if we have used for K_T , the average of all measurements ($K_T = 1.4310 \times 10^{-8}T + 5.8786 \times 10^{-6}$; $R^2 = 0.99994$). It should be stressed that we analyzed the independence on wavelength using gratings inscribed in other fibers and results were even more constant, within 0.001, although for shorter wavelength ranges: SM1500_NA=0.29 (2 FBG; 10 nm), j-fiber SMF (3 FBG; 14 nm), Leoni SMF (5 gratings; 27 nm).

Table 5. $d\lambda/dT$ and K_T values at $20 \text{ }^\circ\text{C}$ obtained using five FBG inscribed in the SMF-28 fiber and Bragg wavelengths fitted in the $[-20, 100] \text{ }^\circ\text{C}$ temperature range.

λ_B (nm)	1509.2	1524.2	1539.2	1554.1	1561.6
$d\lambda/dT$ (pm/ $^\circ\text{C}$)	9.31	9.40	9.49	9.59	9.63
K_T (K^{-1})	6.168×10^{-6}	6.165×10^{-6}	6.165×10^{-6}	6.163×10^{-6}	6.164×10^{-6}

Table 6. Calculated Bragg wavelength and temperature sensitivity for the “unknown” grating.

T ($^\circ\text{C}$)	$\langle\lambda\rangle$ (nm)	$\lambda_{\text{int}2}$ (nm)	$d\lambda_{\text{int}2}/dT$ (pm/ $^\circ\text{C}$)	$d\lambda_{\text{dir}2}/dT$ (pm/ $^\circ\text{C}$)
-20	1561.2157	1561.2133	8.74	8.74
0.1	1561.3939	1561.3934	9.19	9.18
20	1561.5807	1561.5807	9.63	9.63
100	1562.4223	1562.4226	11.42	11.41

Figure 7 shows the wavelength dependence of ‘ K_T ’ for four silica glasses and K_T for five FBG inscribed in the SMF-28 Corning fiber and in the SM1500 fiber (NA=0.19). As can be observed, the wavelength dependence of K_T is negligible for the FBG in the SMF-28 fiber (and also resembles the ‘ K_T ’ behavior of the Corning glass). On the other hand, K_T seems to have a slight dependence on wavelength for FBG in the SM1500 fiber.

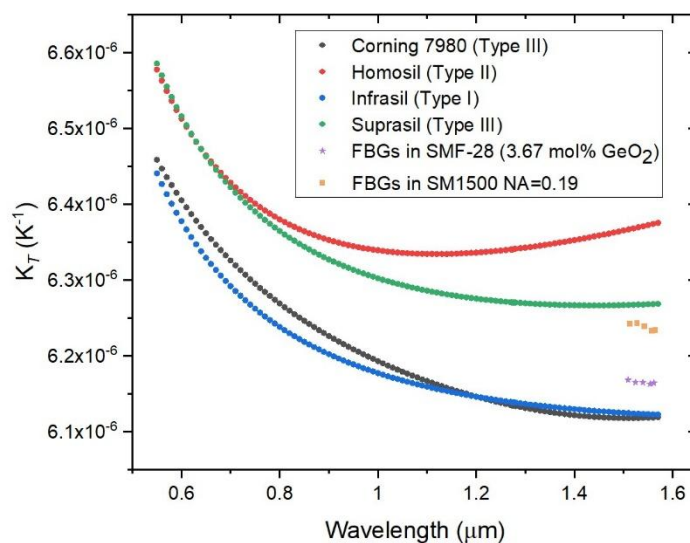


Figure 7. ‘ K_T ’ for four silica glasses [14,23–26] and K_T for UV-FBGs inscribed in the SMF-28 Corning fiber and in FiberCore SM1500 fiber (NA=0.19).

5. Conclusions

We have shown that the temperature dependence of the normalized temperature sensitivity, K_T , was found to be quadratic in the -50 – 200 °C range while it is linear for the -20 – 100 °C range. K_T values at 20 °C range from $5.176 \times 10^{-6} \text{ K}^{-1}$, for a B/Ge co-doped fiber up to $6.724 \times 10^{-6} \text{ K}^{-1}$, for a highly Ge-doped fiber. We have demonstrated that K_T does not depend on the hydrogen-loading process, neither on the gratings coupling strength and that is independent on wavelength in the 1500 – 1600 nm range. Furthermore, gratings produced by femtosecond-laser radiation and UV-laser radiation exhibit comparable values of K_T . The K_T expressions for FBG inscribed in silica fibers with distinct concentrations of GeO_2 was given. A discussion of the potential sources of error on K_T determination was presented. We have introduced a methodology that allows the accurate determination of the temperature dependence of the Bragg wavelength of any grating, as far as one has knowledge of K_T for a single grating inscribed in the same fiber. This methodology is very useful in research labs and computer simulations.

Author Contributions: Conceptualization, methodology and data analysis, G.M.R.; experimental work, J.L.C., M.C., F.M.A., J.P., R.O., R.N., M.P., P.C.; writing—review and editing, G.M.R., J.L.C., and R.O. All authors have read and agreed to the published version of the manuscript.

Funding: This work was financed by national funds through the Portuguese funding agency, FCT – Fundação para a Ciência e a Tecnologia, I.P., under the support of INESC TEC through FCT within project: 10.54499/UID/50014/2025 and supported by The Applied Digital Transformation Laboratory (ADiT-LAB), through FCT within project: 10.54499/UIDP/06121/2025. This work is also funded by FCT – Fundação para a Ciência e a Tecnologia, I.P., and, when eligible, co-funded by EU funds under project/support UID/50008/2025 – Instituto de Telecomunicações, with DOI identifier <https://doi.org/10.54499/UID/50008/2025>. R. Oliveira acknowledges the FCT contract CEECIND2021.01066 with DOI identifier 10.54499/2021.01066.CEECIND/CP1653/CT0004. J. L. Cruz acknowledges the grant through project PROMETEO:CIPROM/2022/30, funded by the Generalitat Valenciana, Spain.

Institutional Review Board Statement: Not applicable.

Informed Consent Statement: Not applicable.

Data Availability Statement: The data segments can be obtained by contacting the corresponding author.

Acknowledgments: Not applicable.

Conflicts of Interest: The authors declare no conflicts of interest.

References

1. Meltz, G., W.W. Morey, and W.H. Glenn, *Formation of Bragg gratings in optical fibers by a transverse holographic method*. Optics Letters, 1989. **14**(15): p. 823-825.
2. Hill, K.O. and G. Meltz, *Fiber Bragg grating technology fundamentals and overview*. Journal of Lightwave Technology, 1997. **15**(8): p. 1263-1276.
3. Kersey, A.D., et al., *Fiber grating sensors*. Journal of Lightwave Technology, 1997. **15**(8): p. 1442-1463.
4. Hill, K.O., et al., *Bragg gratings fabricated in monomode photosensitive optical fiber by UV exposure through a phase mask*. Applied Physics Letters, 1993. **62**(10): p. 1035-1037.
5. Yun-Jiang, R., *In-fibre Bragg grating sensors*. Measurement Science and Technology, 1997. **8**(4): p. 355.
6. Xu, M.G., et al., *Discrimination between strain and temperature effects using dual-wavelength fibre grating sensors*. Electronics Letters, 1994. **30**(13): p. 1085-1087.
7. Sahota, J.K., N. Gupta, and D. Dhawan, *Fiber Bragg grating sensors for monitoring of physical parameters: a comprehensive review*. Optical Engineering, 2020. **59**(6): p. 060901.
8. Iadicco, A., et al., *Self temperature referenced refractive index sensor by non-uniform thinned fiber Bragg gratings*. Sensors and Actuators B: Chemical, 2006. **120**(1): p. 231-237.

9. Lobry, M., et al., *Plasmonic Fiber Grating Biosensors Demodulated Through Spectral Envelopes Intersection*. Journal of Lightwave Technology, 2021. **39**(22): p. 7288-7295.
10. Feng, D., et al., *High-Precision Temperature-Compensated Magnetic Field Sensor Based on Optoelectronic Oscillator*. Journal of Lightwave Technology, 2021. **39**(8): p. 2559-2564.
11. Zhao, Y. and Y. Liao, *Discrimination methods and demodulation techniques for fiber Bragg grating sensors*. Optics and Lasers in Engineering, 2004. **41**(1): p. 1-18.
12. Kinet, D., et al. *Fiber Bragg Grating Sensors toward Structural Health Monitoring in Composite Materials: Challenges and Solutions*. Sensors, 2014. **14**, 7394-7419 DOI: 10.3390/s140407394.
13. Rego, G.M. *Temperature Dependence of the Thermo-Optic Coefficient of GeO₂-Doped Silica Glass Fiber*. Sensors, 2024. **24**, DOI: 10.3390/s24154857.
14. Rego, G. *Temperature Dependence of the Thermo-Optic Coefficient of SiO₂ Glass*. Sensors, 2023. **23**, DOI: 10.3390/s23136023.
15. Flockhart, G.M.H., et al., *Quadratic behavior of fiber Bragg grating temperature coefficients*. Applied Optics, 2004. **43**(13): p. 2744-2751.
16. João, P., et al. *Normalized temperature sensitivity of fiber Bragg gratings inscribed under different conditions*. in Proc.SPIE. 2025.
17. Imas, J.J., et al., *Accurate compensation and prediction of the temperature cross-sensitivity of tilted FBG cladding mode resonances*. Applied Optics, 2023. **62**(16): p. E8-E15.
18. Wenyuan, W., et al. *Measurements of thermo-optic coefficient of standard single mode fiber in large temperature range*. in Proc.SPIE. 2015.
19. Tan, C.Z., *Dependence of the refractive index on density, temperature, and the wavelength of the incident light*. 2021. **94**: p. 139.
20. Rego, G.M., *Arc-induced long-period fibre gratings : fabrication and their applications in optical communications and sensing*, in Engineering Faculty. 2006, Porto: Porto University.
21. Rego, G., et al., *New technique to mechanically induce long-period fibre gratings*. Optics Communications, 2003. **220**(1-3): p. 111-118.
22. Colaço, C., et al., *Arc-Induced Long-Period Fiber Gratings in the Dispersion Turning Points*. Journal of Lightwave Technology, 2016. **34**(19): p. 4584-4590.
23. Leviton, D.B. and B.J. Frey. *Temperature-dependent absolute refractive index measurements of synthetic fused silica*. in Proceedings of SPIE - The International Society for Optical Engineering. 2006.
24. Leviton, D.B., B.J. Frey, and T.J. Madison. *Temperature-dependent refractive index of CaF₂ and Infrasil 301*. in Proceedings of SPIE - The International Society for Optical Engineering. 2007.
25. Leviton, D.B., et al. *Temperature-dependent refractive index measurements of CaF₂, Suprasil 3001, and S-FTM16 for the Euclid near-infrared spectrometer and photometer*. in Proceedings of SPIE - The International Society for Optical Engineering. 2015.
26. Miller, K.H., M.A. Quijada, and D.B. Leviton. *Cryogenic refractive index of Heraeus homosil glass*. in Proceedings of SPIE - The International Society for Optical Engineering. 2017.

Disclaimer/Publisher's Note: The statements, opinions and data contained in all publications are solely those of the individual author(s) and contributor(s) and not of MDPI and/or the editor(s). MDPI and/or the editor(s) disclaim responsibility for any injury to people or property resulting from any ideas, methods, instructions or products referred to in the content.